

Analysis of Seismogenic Perturbations using Bartlett Method for Earthquake Signatures on GPS TEC

Ch. Goutham, K. Rakesh, K. S. Ramesh, R. Revathi and S. Koteswra Rao P. Chitra and V. N. Ramakrishnan

Guntur, Andhra Pradesh, India; cgoutham101@gmail.com, rakesh.ranjith34@gmail.com, dr.ramesh@kluniversity.in, revathimouni@gmail.com, rao.sk9@gmail.com

Abstract

Background/Objectives: Earthquakes are the most unpredictable natural disasters in nature. Spectral analysis of seismo-ionospheric perturbations will be helpful in understanding the source mechanisms of the earthquakes. Seismogenic perturbations observed in ionosphere for an earthquake occurred on 19th December 2013 are investigated. The earthquake peaked at 4.6 on Richter scale. It took place at 16:41 hour's green which mean time. International global navigation satellite services data for the station BAKO is considered for the analysis. **Methods/Statistical Analysis:** In present work Bartlett method is implemented on the vertical total electron content data on the earthquake day. **Findings:** Earthquake signatures in the ionosphere are indentified. It is also observed that the power spectral density of the perturbations has a giant initial value and abated slowly. **Application:** These findings will aid us to develop early warning systems for earthquakes.

Keywords: Earthquake, Signal Processing, Upper Atmospheric Sciences

1. Introduction

The advancement in the satellite technology has unraveled many physical phenomenons occurring in the earth's atmosphere. Remote sensing of earth and its related systems is useful in experimentation of the scientific hypothesis of natural disasters. Global Positioning System (GPS) has played an crucial role in understanding and explaining the coupling mechanisms of lower and upper atmospheres and lithosphere^{1,2}.

Pulinets has categorically explained the coupling between ionosphere and seismicity. These investigations started from the Great Alaskan earthquake occurred on 27th March 1964. Different theories were which explained the generation of anomalous vertical electric field during and before its occurrence due to the release of radioactive elements from the earths crust leading to generation of radon ions. The anomalous electric field perturbs the ionosphere resulting in seismo ionospheric perturbations. The perturbations observed in the ionosphere are in accordance with

the lithosphere-atmosphere - ionosphere coupling mechanisms³⁻⁷.

The ionospheric refractive index induces time delay in the GPS signals navigating through it. The additional time delay is measured as the difference in the number of cycles received by the ground based GPS receiver. This will be equal to the integral number of electrons present in the line of sight path between the receiver and the satellite represented by S_1 . The induced time delay measured in meters is called as pseudorange. The pseudorange measured in meters for a single frequency GPS receiver ' α_1 ', is given by

$$\alpha_1 = (40.3 * S_1) / f_1^2 \quad (1)$$

For a GPS receiver of dual frequency, it is given by

$$\alpha_1 - \alpha_2 = (40.3 * S_1) * [(1/f_1^2) - (1/f_2^2)] \quad (2)$$

where f_1, f_2 correspond to GPS L₁, L₂ signals respectively. For a dual frequency GPS receiver S_1 is given by

*Author for correspondence

$$S_1 = \left[\frac{(\rho_1 - \rho_2)}{40.3} \right] * \left[\frac{f_1^2 * f_2^2}{f_1^2 - f_2^2} \right] \quad (3)$$

The GPS receiver archives S_1 values as the satellite is moving over the specific location. The total electron content straight above the GPS receiver is calculated by taking the product of S_1 and the cosine of the difference between 90° and the satellite zenith angle at a height of 350km. It is given by

$$V_1 = S_1 (\cos(\beta)) \quad (4)$$

The V_1 data is collected from the single GPS receiver is analyzed in the present research work. The uniqueness of the work is 1. The data does not contain huge modeling errors 2. Data is recorded at equal time intervals. This assists in the exertion of the spectral estimation techniques on GPS TEC⁸.

2. Event Considered

On 19th December 2013, a massive earthquake (EQ) took place in ciranjang-hilir, Indonesia which is located at 6.812° south latitude and 107.96° east longitude. The quake occurred at 16:41 hours UTC i.e. at 10:11 hours LTC. The earthquake recorded peak amplitude of 4.6 on the Richter scale. The location map of the earthquake is taken from the website (<http://earthquaketrack.com/quakes/2013-12-19-16-41-49-utc-4-6-135>) which is given in Figure 1.

3. Data

There are more than 200+ GPS receivers all over the world. The data of these GPS receivers (V_1) is maintained by the International Global Navigation Satellite Systems (IGS). In Bakosurtanal, West Java, an IGS station named BAKO is present from which the V_1 data is taken for analysis. According to GPS calendar earthquake occurred on 353rd day of the year 2013. It is clearly detected that the V_1 data of GPS satellite number 18 is disrupted on EQ day. V_1 data on EQ day and the corresponding satellite ray path with respect to time is given in Figure 2 and Figure 3.

4. Methodology

From Figure 2, it is clearly pinpointed that V_1 data is disrupted for 120 minutes during the occurrence of the

perturbation i.e. from 11:58 hours to 13:58 hours in Indonesia. V_1 data of the GPS satellite number 18 is available from 11:58 21:36 hour's local time. V_1 data of satellite number 18 is not visible ahead of the time from where the data is recorded. So, the V_1 is bisected into perturbed and unperturbed parts. The undisturbed data is considered up to 17 hours LTC only. Because after that time, there will be post sunset disturbances. The V_1 data consists 1038 points. The disturbed and undisturbed data sets consist of 202 points and 299 points respectively.

There are many methods to identify disturbances in the signals⁹⁻¹². For earthquake day data, Bartlett a non parametric method is used to realize the seismogenic perturbation in ionosphere. These methods estimate the signal below detection level. They do not assign arbitrary values to the data below detection level. The specified method estimates the spectrum by taking the ensemble averages of the time series data. The advantage of this method is that the variance if the data record is reduced. A signal $x(n)$ having frequencies 0.15 and 0.8 is developed in matlab. It is represented as

$$x(n) = 2\cos(2\pi f_1 n) + 2\cos(2\pi f_3 n) + c(n) \quad (5)$$

where $f_1 = 0.15$ and $f_3 = 0.8$, $c(n)$ is zero mean white Gaussian noise, $n = 0$ to $N-1$ and N is the number of FFT points. Bartlett algorithm is first realized for the synthetic signal. The spectral density (P_1) of synthetic signal is shown in Figure 4. It is clearly observed that the peaks are seen at frequencies of 0.15 and 0.8. Hence the algorithm is enforced on the perturbed and unperturbed V_1 data on EQ day.

The detrended perturbed and unperturbed data are given in Figure 5 (a) and (b). P_1 of the perturbed and unperturbed VTEC are shown in Figure 6 (a) and (b). In the P_1 of the disturbed V_1 peaks are seen at normalized frequencies 0.3438, 0.5781, 0.7656 and 0.9141 with P_1 of 23.6dB, 19.33 dB, 20.97 dB and 20.08 dB respectively. No peaks are observed in undisturbed V_1 .

Multi resolution analysis is carried on the disturbed V_1 to increase the confidence bounds in the time of occurrence of the perturbations. So, the V_1 data is sliced into sets of 100 and 50 data points each. In the first bisection of V_1 data into sets 100 points each. A peak is noticed in the first set at normalized frequency 0.4844 with P_1 of 20.08 dB and in the second set peaks are seen at normalized frequencies 0.4922 and 0.7813 with P_1 's of 7.111 dB and

-1.336 dB respectively. The P_1 plot for the first division is represented in Figure 7.

In the last division of V_1 into 50 points, peaks are examined in first three sets of at normalized frequencies 0.4922, 0.8125 and 0.4609 with P_1 's of 20.14 dB, 12.99 dB and 1.808 dB respectively. This shows that there is a clear difference in the energy of the ionosphere during the occurrence of the perturbations and unperturbed data. In the last breakup of V_1 into 50 points each it is observed that the P_1 had a negative value. This represents that the energy in the ionosphere has decreased at that time. The plot of second division of V_1 into 50 data points is represented in Figure 8. The BAKO station is 184.5 km from the epicenter. Thus, it may be concluded that the perturbations seen are due to the impending earthquake.

5. Conclusions

The analysis of V_1 using Bartlett method was able to identify seismic perturbation in ionosphere. The research work shows that there is a deportation and relocation of ions in the ionosphere leading in to a definite change energy and momentum from lower to upper atmosphere before, during and after the occurrence of the earthquake. Thus it may be stated that if we have sufficient data set for three to five days, round the clock before and after the occurrence of the earthquake, short term precursors can be thoroughly analyzed to identify earthquake signatures in ionosphere.

6. Acknowledgments

This research work is supported by the Department of Science and Technology (DST), Government of India via sponsored projects SR/AS-04/WOS-A/2011 and SR/S4/AS-9/2012. The authors would like to thank the DST panel of Atmospheric Sciences and President, Koneru Lakshmaiah University for their continuous support and encouragement.

7. References

- Akyol AA, Arıkan O, Feza Arıkan M, Deviren N. Investigation on the reliability of earthquake prediction

based on ionospheric electron content variation. 16th IEEE International Conference on Information Fusion (FUSION); 2013. p. 1658–63. ISBN: 978-605-86311-1-3.

- Komjathy A. Global ionospheric total electron content mapping using the global positioning system [PhD dissertation]. New Brunswick, Canada: Department of Geodesy and Geomatics Engineering, University of New Brunswick, Fredericton; 1997. 248 pp.
- Sergey P. Ionospheric precursors of earthquakes. Recent Advances in Theory and Practical Applications. Sep 2004; 15(3):413–35.
- Thanassoulas C, Tselentis G. Periodic variations in the Earth's electric field as earthquake precursors: Results from recent experiments in Greece. Tectonophysics. 1993; 224:103–11.
- Freund F. Cracking the code of pre-earthquake signals. National Information Service for Earthquake Engineering, Berkeley: University of California; 2005. Available from: <http://solarcenter.stanford.edu/SID/educators/earthquakes.html>
- Gosh D, Midy SK. Associating an ionospheric parameter with major earthquake occurrence throughout the world. Journal of Earth Systems and Science. Feb; 123(1):63–71.
- Ouzounov D, et al. Atmosphere-ionosphere response to the M9 Tohoku earthquake revealed by joined satellite and ground observations. Preliminary Results. DOI: 10.1007/s11589-011-0817-z. Available from: arxiv.org/abs/1105.2841
- Mishra P. Global positioning systems. 2nd ed. Ganga-Jamuna Press.
- Jagan OL, Koteswara Rao S, Jawahar A, Karishma SKB. Application of particle filter using bearing measurements. Indian Journal of Science and Technology. 2016 Feb; 9(7):1–4.
- Jawahar A, Koteswara Rao S. Recursive multistage estimator for bearings only passive target tracking in ESM EW Systems. Indian Journal of Science and Technology. Oct 2015; 8(26):74932.
- Annabattula J, Koteswara Rao S, Sampath Dakshina Murthy A, Srikanth KS, Das RP. Multi-sensor submarine surveillance system using MGBEKF. Indian Journal of Science and Technology. Dec 2015; 8(35). DOI: 10.17485/ijst/2015/v8i35/82088.
- Mylapilli NS, Koteswara Rao S, Das RP, Raju L. Underwater target tracking using unscented Kalman Filter. Indian Journal of Science and Technology. Nov 2015; 8(31). DOI: 10.17485/ijst/2015/v8i31/77054.

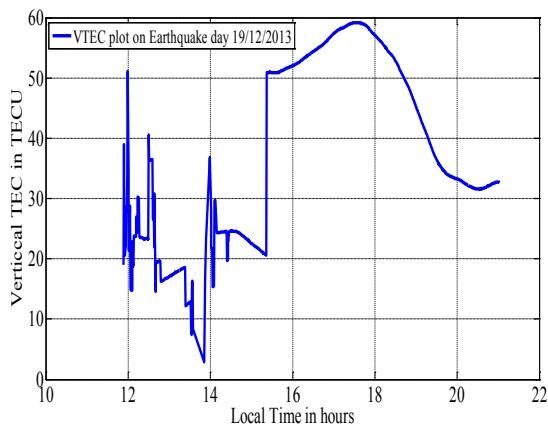


Figure 1. Location map of the EQ.



Figure 2. V1 of PRN 18 on EQ day.

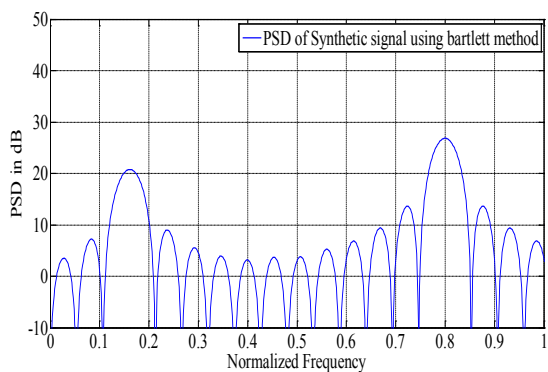


Figure 3. Satellite ray path for PRN 18.

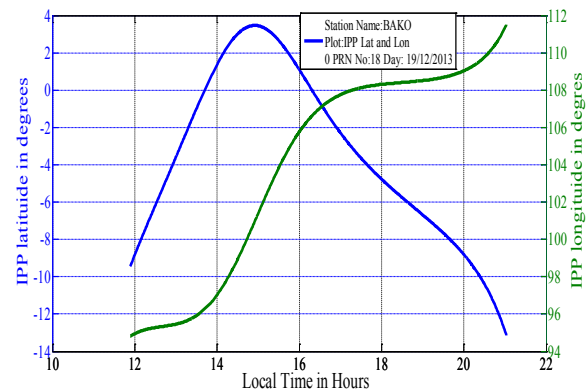
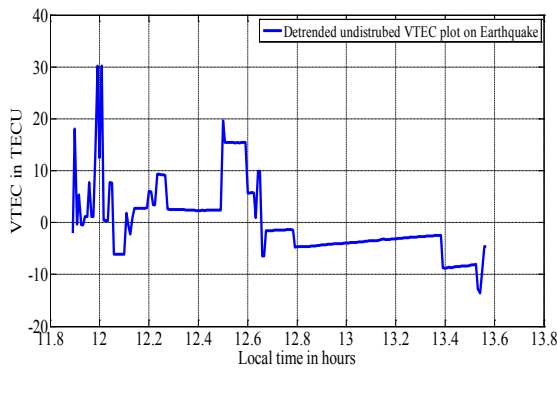
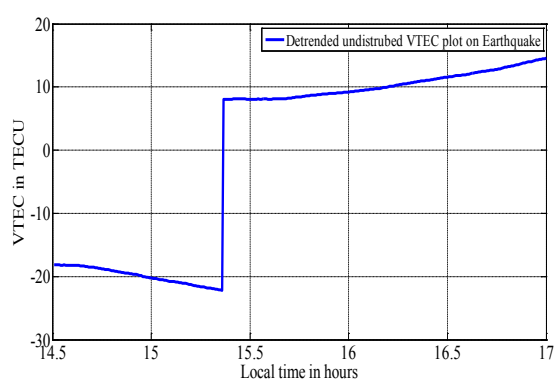


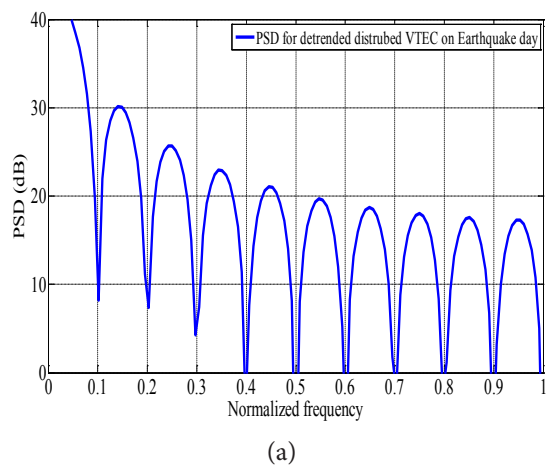
Figure 4. P_1 of synthetic signal using Bartlett method.



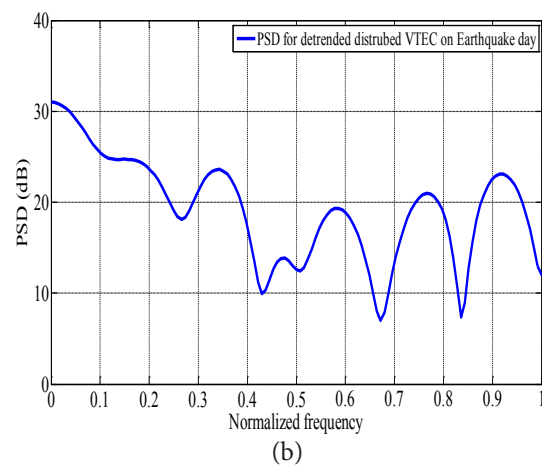
(a)



(a) (b)



(a)



(b)

Figure 6. (a) and (b) are P_1 's of detrended disturbed and undisturbed V_1 on the earthquake day.

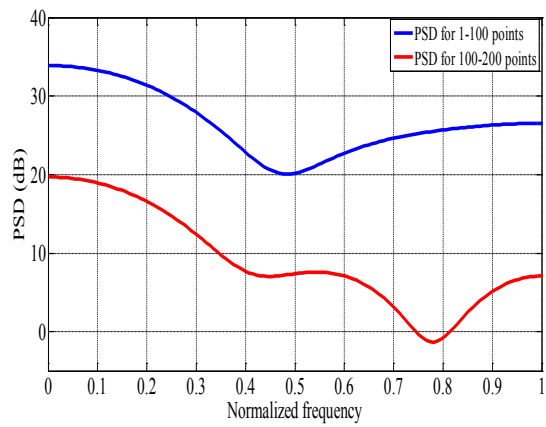


Figure 7. P_1 of disturbed V_1 for 100 points each.

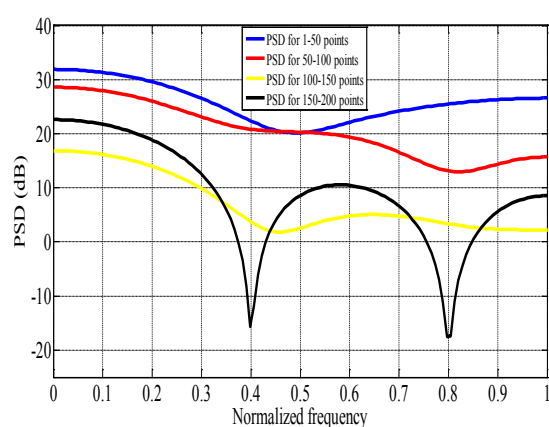


Figure 8. P_1 of disturbed V_1 for 50 points each.